Improvements on an analytical representation of the polarized HERA beam

Thomas Boyer

23 July 2021

Abstract

In this memo we present improvements on an analytical approximation of a simulation of the beam of the HERA dishes developed in [Fag+20] *via* a CST simulation. We build upon the approximation developed in [CBK20], focusing mainly on the incorporation of polarization effects, and seeking a better fit of the various components of the electric field and the derived power beams. We find that, by modulating the existing analytical approximation with an adjusted dipole matrix, we are able to recover polarization structure for the E-fields, and that the derived power beams show decent fitting. Weighted normalized differences with the reference beam are in the 5-25% range.

Contents

1 Introduction

In [CBK20], efficient[1] analytical representations of the (azimuthally-averaged) pseudo-Stokes I Fagnoni beam at 100 MHz were found. They consist in functional bases of Chebyshev polynomials that were selected against other families of polynomials for offering the best compromise between accuracy and succinctness in the number of parameters. An attempt to fitting this very beam at higher frequencies (up to 200 MHz) was also made by adding a power law in frequency scaling the zenith angle (resulting in a contraction of the beam at higher frequencies). The derived `PolyBeam` E-field obtained with these parameters is the square-root of that fitted power beam, thus lacking cross-polarization and imaginary components[2]. Hence, it does not adequately model the different polarizations of the "original" E-field, as shown in figure 1.
Note that in this memo, the HERA beam of reference, "the Fagnoni beam", was downloaded from the `hera_pspec` GitHub repository in the form of a `beamfits` file, and peak normalized.

[1] *i.e.* depending on few coefficients (typically ~ 20).
[2] as the pseudo-Stokes Fagnoni power beam is itself real.

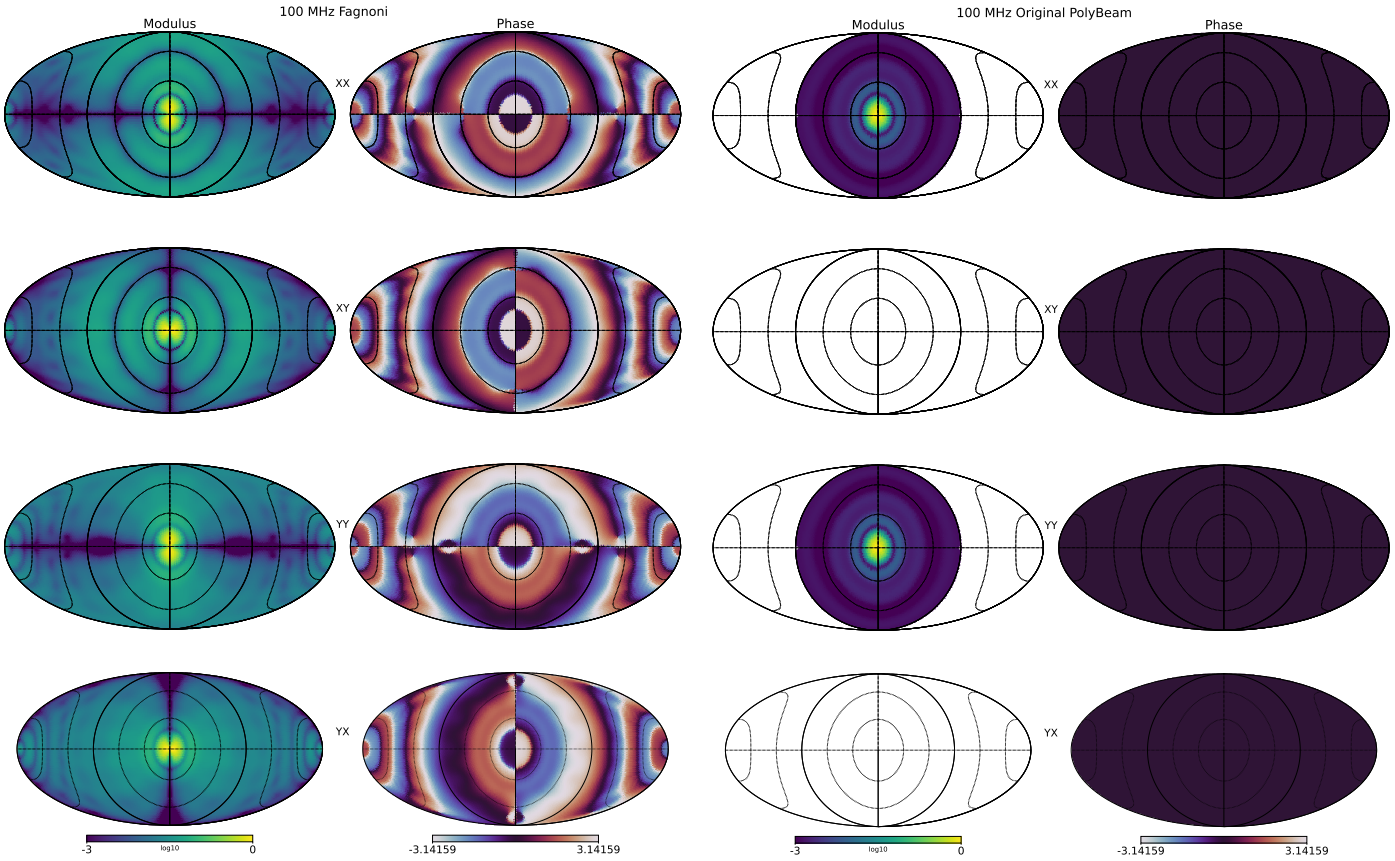

(a)

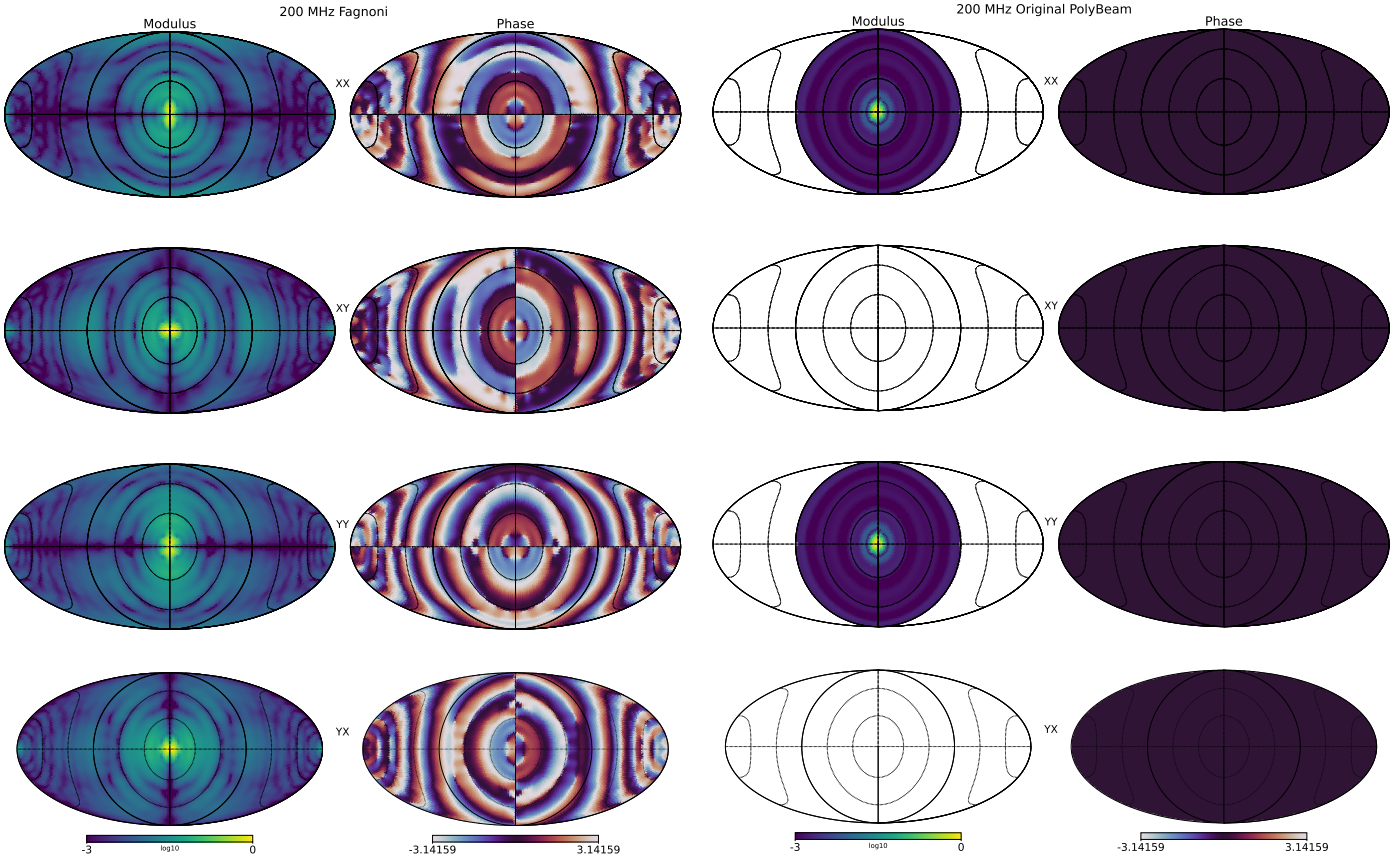

(b)

Figure 1: Modulus ($\log_{10}$) and phase of X/Y polarizations of the Fagnoni E-field beam (left), and of the PolyBeam (right) at 100 MHz (up), and 200 MHz (down).

2 Polarization-related changes to `PolyBeam`

In order to take into account the polarized nature of the *true* beam, and its best representation at our disposal in the form of the Fagnoni beam, we modulate the original unpolarized PolyBeam with a polarized dipole pattern.
More specifically, we multiply the beam pattern with a zenith–and–azimuth–dependent complex dipole matrix $\mathcal{M}$:

$$\mathcal{M} = \mathrm{q}(\theta_s) \times \big(1 + \mathrm{p}(\theta_s) \times i\big) \times \begin{bmatrix} -\sin(\phi) & \cos(\phi) \\ \cos(\phi) & \sin(\phi) \end{bmatrix} \tag{1}$$

where i is the imaginary unit, θ_s is the stretched zenith angle, ϕ the azimuth angle, p and q are the functions defined *ad hoc* by:

$$\mathrm{p}(\theta_s) = \begin{cases} 0 & \text{if } \theta_s < \frac{\pi}{11} \\ \pi \sin(\pi\theta_s) & \text{otherwise} \end{cases} \quad \text{and} \quad \mathrm{q}(\theta_s) = \begin{cases} i & \text{if } \frac{\pi}{6} > \theta_s > \frac{\pi}{11} \\ 1 & \text{otherwise} \end{cases} \tag{2}$$

and the stretched zenith angle θ_s is $\theta_s = \theta \times \left(\frac{f}{f_{\text{ref}}}\right)^{-\beta}$, that is the zenith angle θ divided by the power law defined in [CBK20]. The p function was introduced as an attempt to reproduce both the general behavior of the phase of the Fagnoni beam (the $\sin$ part) and the "first ring" (the $\theta < \frac{\pi}{11}$ region), while the q function specifically renders the "second ring" (the $\frac{\pi}{6} > \theta > \frac{\pi}{11}$ region). The stretching of the zenith angle had to also be added here since the original code does not take into account the phase component.
We then attempt to further match the frequency-dependent behavior of the Fagnoni beam by shifting the phase of the resulting PolyBeam. We do this, again *ad hoc*, by subtracting an affine function of frequency to the phase of the PolyBeam:

$$\text{phase}(\mathcal{B}) \longmapsto \text{phase}(\mathcal{B}) - \frac{\pi(f - f_{\text{ref}})}{18 \text{ MHz}} \tag{3}$$

where $\mathcal{B}$ is the complex beam at any given frequency and polarization, and f and f_{ref} are respectively the frequency at which the beam is computed and the reference frequency for the beam width scaling power law. The resulting phase is then wrapped to $[-\pi, \pi]$, following the Fagnoni beam's convention.
Finally, we scale the modulus of that newly polarized PolyBeam by elevating it to an *ad-hoc* power exponent of 0.6, so that it fits better the Fagnoni beam, and especially the azimuthally-averaged power beams shown in figure 7.

3 Fitting to the reference Fagnoni beam

We chose to work with the parameters[3] described in [Gar] that were obtained by fitting the square root of the Fagnoni beam, and instantiate a `PolyBeam` object with the following parameters:

```
ref_freq = 1e8
spectral_index = -0.6975
beam_coeffs =    [ 2.35088101e-01, -4.20162599e-01,  2.99189140e-01, -1.54189057e-01
  3.38651457e-02,  3.46936067e-02, -4.98838130e-02,  3.23054464e-02, -7.56006552e-03,
 -7.24620596e-03,  7.99563166e-03, -2.78125602e-03, -8.19945835e-04,  1.13791191e-03,
 -1.24301372e-04, -3.74808752e-04,  1.93997376e-04, -1.72012040e-05]
polarized = True
```

using the `viscpu_pol` branch of `hera_sim`, where `spectral_index` is the power exponent of the power law (denoted β beforehand).

3.1 E-fields

We decide to consider the modulus and phase of the E-fields rather than their real and imaginary part as the polar representation offers vastly more structure than the Cartesian one. Since each polarization shows quite different structure, we hence further differentiate them, allowing us to independently compare the hoped-for improvements on each polarization.
Figure 2 shows this polarized PolyBeam in orthographic projection at 100 MHz (where the fit is the best) and 200 MHz, alongside the reference beam. One can see that the polarized version now shows proper structure for each polarization and scalar component, and that the dipole–like structure of the Fagnoni beam –especially seen at the center– is better approximated. The fitting clearly degrades with frequency, especially for the phase.

[3] 18 polynomial coefficients, a reference frequency and a spectral index.

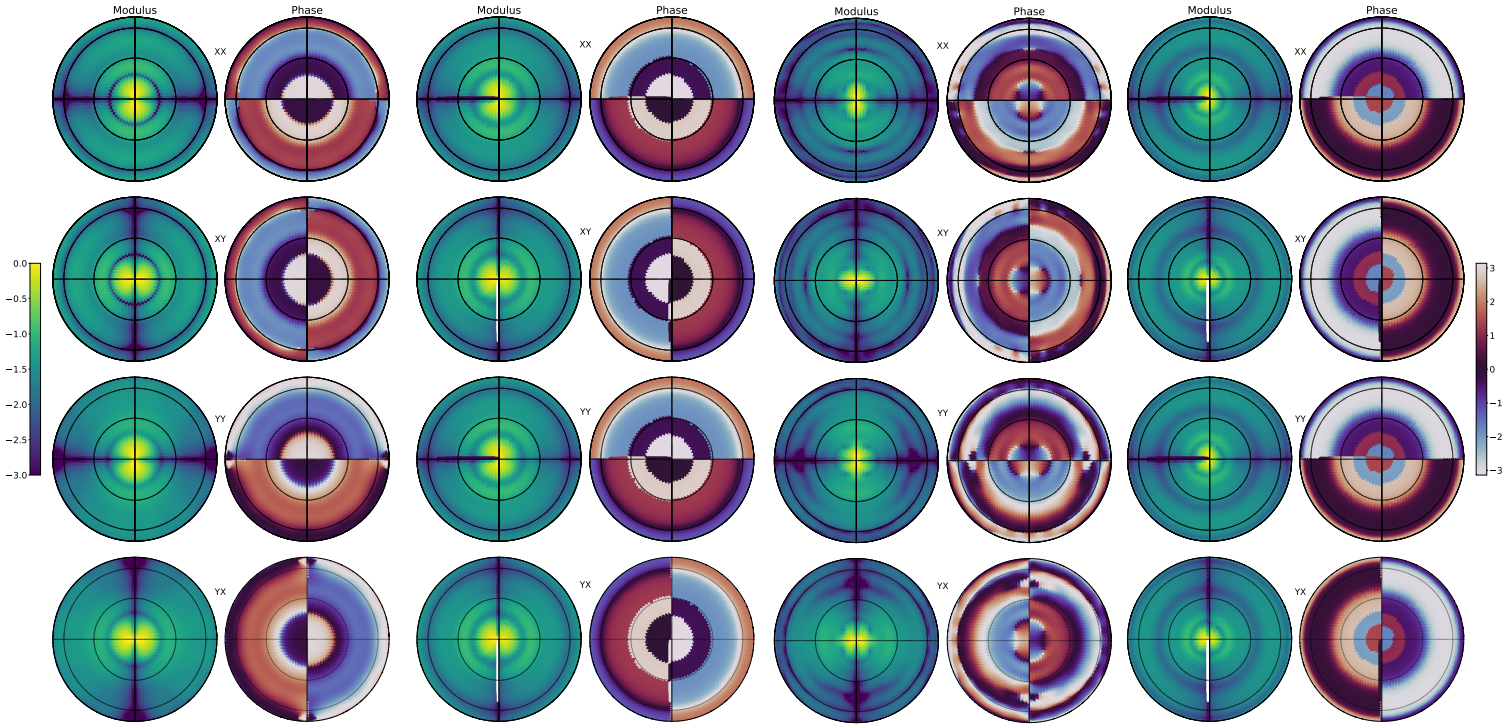

(a) Fagnoni, 100 MHz (b) Polarized PolyBeam, 100 MHz (c) Fagnoni, 200 MHz (d) Polarized PolyBeam, 200 MHz

Figure 2: X/Y polarizations of the E-fields in orthographic projection. Only the "upper" hemisphere is shown.

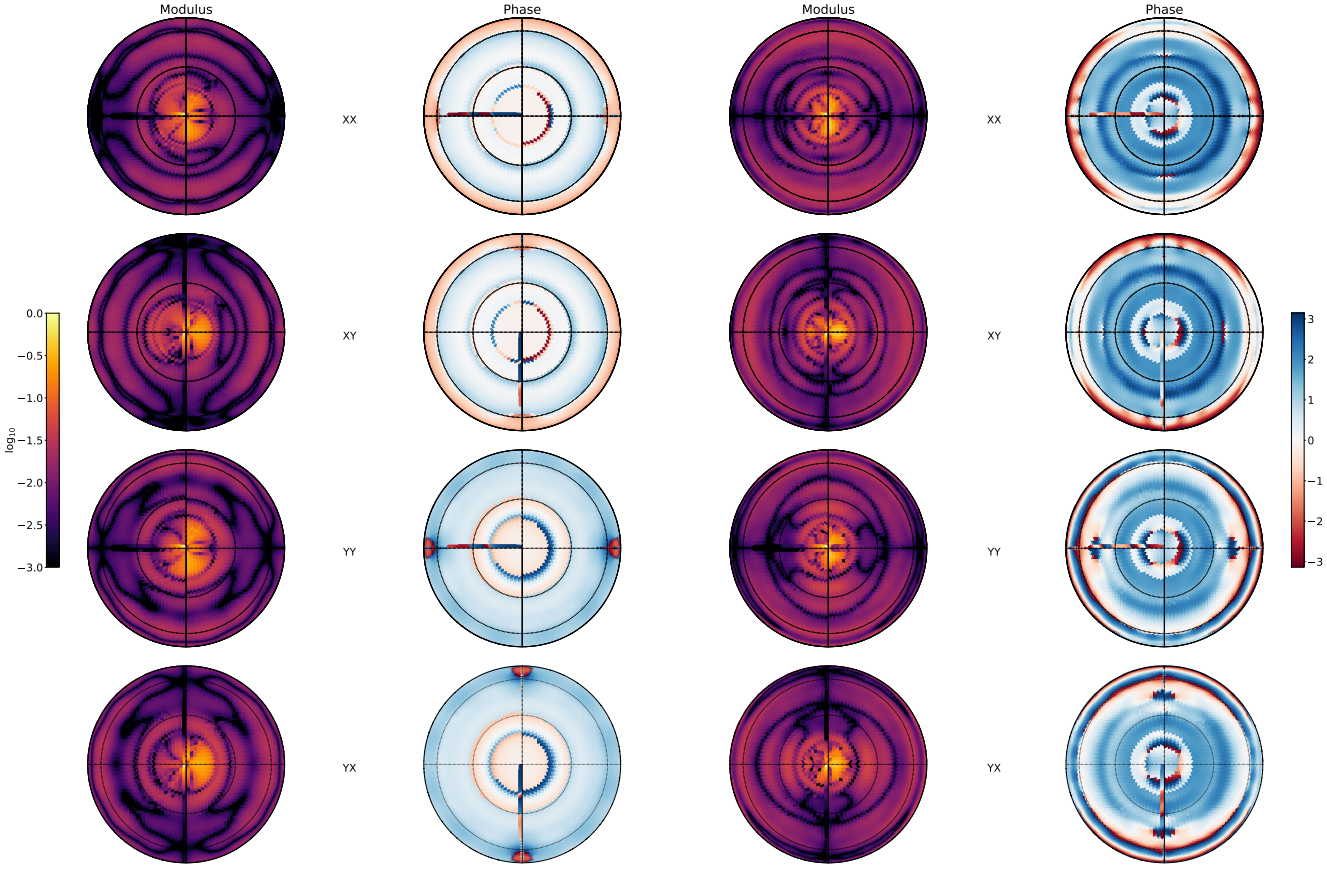

Figure 3: Absolute difference of the modulus ($\log_{10}$) and difference of the phase of X/Y polarizations of the Fagnoni beam and the polarized PolyBeam at 100 MHz (left) and 200 MHz (right). Hemispherical orthographic projection.

However, the phase of the beam, although showing complex structure –especially at high frequency– is quite well approached in the center, where the modulus of the E-field is the greater.
In figure 3 we plot the difference of these beams. Note that the difference between the modulus is actually the $\log_{10}$ of the absolute difference, and that the difference of the phases is always wrapped back to $[-\pi, \pi]$. It reveals clearly

that some phase structure, especially at high frequencies, is still unmatched, and that systemic offsets of the modulus still exist (note that a higher difference in the center is also associated with higher values of the beam).
Since the beams studied here are complex 2D spherical maps depending on polarization and frequency, this would give us 208 2D scalar maps to compare for the raw E-fields, and 104 for the pseudo-Stokes power beams[4]. Therefore, we obviously need to summarize their difference. Let us first try to compare the raw E-fields. We plot measurements, aggregated over the sphere, of the fitting of the polarized PolyBeam to the Fagnoni beam along frequency, by far the smoothest axis of our data. The results we obtain depend of course on the metric used to compare the beams.

3.1.1 Hemispherical weighted mean and median deviation

We plot the upper hemispherical weighted mean and median deviation along frequency, that is:

$$\left\langle 1 - \frac{\text{PolyBeam}}{\text{Fagnoni}} \right\rangle_{\text{W}} \tag{4}$$

where "PolyBeam" or "Fagnoni" denotes the eponym beam on the $\theta \in [0, \frac{\pi}{2}]$ "upper hemisphere" region, at a given frequency and polarization, and $\left\langle \cdot \right\rangle_{\text{W}}$ represents either the mean or the median, computed over all the hemisphere, and weighted either by a "0-1" function χ selecting a part of the hemisphere with lower θ angles than a certain θ_{cut}, or by the very values of the modulus of the Fagnoni beam, noted |Fagnoni|, at the corresponding frequency and polarization, that is:

$$\langle X \rangle_{\text{W}} = \left\langle X \times \frac{\chi(\theta < \theta_{\text{cut}})}{\Sigma} \right\rangle \qquad \text{or} \qquad \langle X \rangle_{\text{W}} = \left\langle X \times \frac{|\text{Fagnoni}|}{\Sigma} \right\rangle \tag{5}$$

where Σ is the sum of the weights, and all operations happen element-wise[5].
The smaller θ_{cut} is, the less we take into account the outer lobes of the beams, where the fit is less convincing, but also where the beam itself is closer to zero. We also chose to take the modulus of the Fagnoni beam itself as a weighting because it does indeed represent the sensibility of the array, better than a simpler Gaussian filter for example.
In figure 4 we plot this metric (in percentage) for each polarization, frequency and polar coordinate, and for different weightings for the modulus only, as different weightings did not output significantly different results for the phase. The numbers obtained are usually in the 10% range, but with high variability. Globally, and as expected, tighter weighting around the center gives lower deviations. The median value is also often lower than the mean one, indicating that outliers perturb the averaging. The median phase component for example shows good results, below 10%, for the XX and YY polarizations below 132 MHz, and the median modulus component of the XY and YX polarization, is almost always 10% throughout the frequency range with the Fagnoni weighting.

3.1.2 Hemispherical weighted normalized distance

Another metric would be the weighted normalized *distance* (still computed within the upper hemisphere only), that is:

$$\frac{\|\text{Fagnoni} - \text{PolyBeam}\|_{\text{W}}}{\|\text{Fagnoni}\|} \tag{6}$$

where $\|\cdot\|$ denotes the euclidean vector 2-norm and $\|\cdot\|_{\text{W}}$ the weighted one, defined by:

$$\|X\|_{\text{W}} = \left\| X \times \frac{\chi(\theta < \theta_{\text{cut}})}{\Sigma} \right\| \qquad \text{or} \qquad \|X\|_{\text{W}} = \left\| X \times \frac{|\text{Fagnoni}|}{\Sigma} \right\| \tag{7}$$

This metric is shown in percentage in figure 5. The distance reveals in a clearer way the effect of the weighting, strongly enhancing the numbers with the Fagnoni weighting compared to the $\theta_{\text{cut}} = \pi/3$ one. The normalized distance weighted with the actual Fagnoni beam shows consistent values in the 15-25% range for the modulus, and 5-20% for the phase.
It must be noted that, for the same weighting, the polarized version systematically achieves better results than the original one where it exists (so for the modulus of two polarizations), meaning that not only did we not alter the "existing fit", but we actually improved it[6].

[4] 26 frequencies (those of the Fagnoni beam), 1 or 2 scalar component(s), 4 polarizations.
[5] That is, pixel-by-pixel.
[6] Note that fitting the E-field was not the purpose of the original PolyBeam.

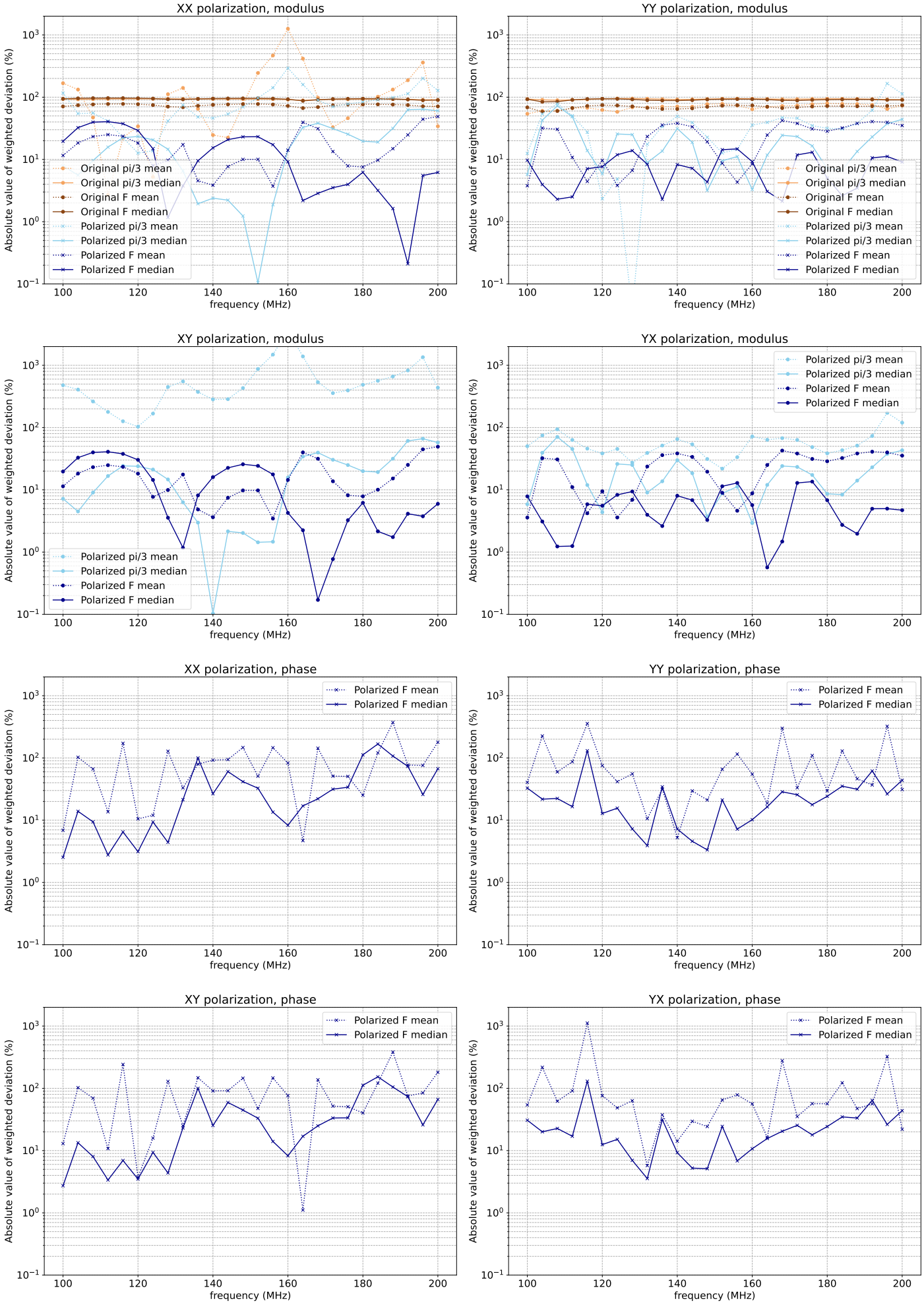

Figure 4: Modulus and phase of the absolute value of the upper hemispherical weighted mean and median deviation for the 4 linear polarization for the polarized PolyBeam (blue), and the original one (orange) where it is non-null, along frequency.

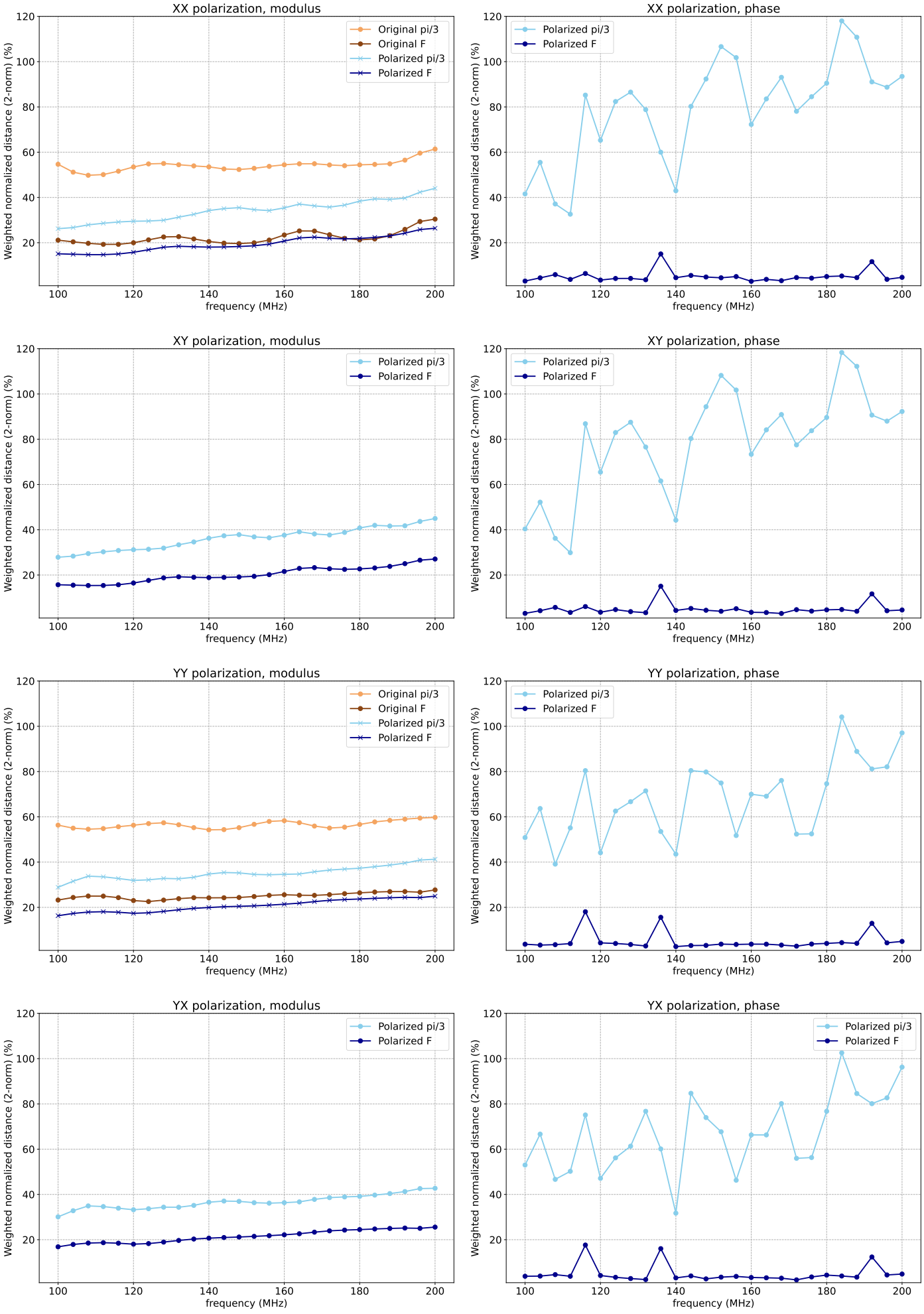

Figure 5: Modulus and phase of the upper hemispherical normalized distance for the 4 linear polarization for both the original PolyBeam (orange) where it exists and the polarized one (blue) along frequency.

3.2 Power fields

Let us now explore what changes were passed on to the power beams, after having modified the raw E-fields as described earlier. We use the "same", slightly adapted source code to derive the pseudo-Stokes power beams from our `PolyBeam` object as the `pyuvdata` library, used for the Fagnoni beam, notably directly re-using the basis vector of the Fagnoni beam. In figure 6 we plot hemispherical orthographic projections of the pseudo-Stokes power fields for the Fagnoni and polarized PolyBeam at extremal frequencies. The original PolyBeam (not shown here) consists only in a fit of the pI Fagnoni beam at 100 Mhz, and lacks some structure observed in the reference beam that is however seen in the Polarized version. It is also clear that, like for the modulus of the E-fields described earlier, a systematic offset appears at high frequencies in the outer lobes of the hemisphere.

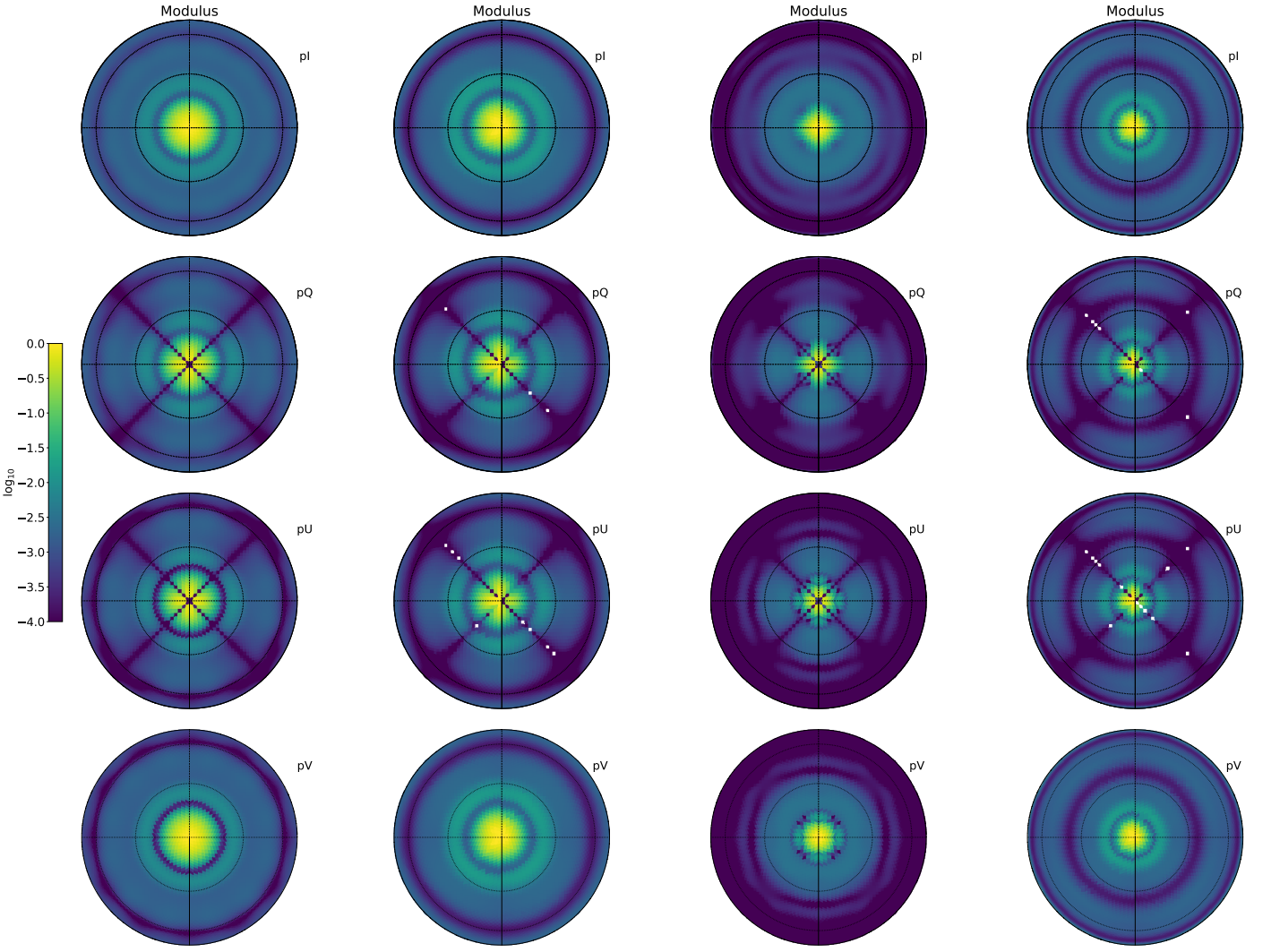

(a) Fagnoni, 100 MHz (b) Polarized PolyBeam, 100 MHz (c) Fagnoni, 200 MHz (d) Polarized PolyBeam, 200 MHz

Figure 6: Pseudo-Stokes power fields ($\log_{10}$)

3.2.1 Azimuth averaging

To further compare the highly azimuthally-symmetric power beams, we average them along the ϕ axis at a given θ value, and represent them against the reference Fagnoni beam in figure 7, at selected frequencies, for the 4 polarizations. The original PolyBeam fits perfectly the pseudo-Stokes I Fagnoni beam at 100 MHz, as expected. It is clear that more than a simple power scaling law is still needed to take into account the variations of the Fagnoni power field at higher θ angle along frequency, however these variations are of very low magnitude compared to the values of the low θ region. The polarized PolyBeam power beams show decent fitting at pQ, pU and pV polarizations of the corresponding Fagnoni beams up to 0.3 or 0.5 rad, thanks only to the newly polarized E-field from which these power beams were computed, thus validating that the power beams are also consistent with the reference.

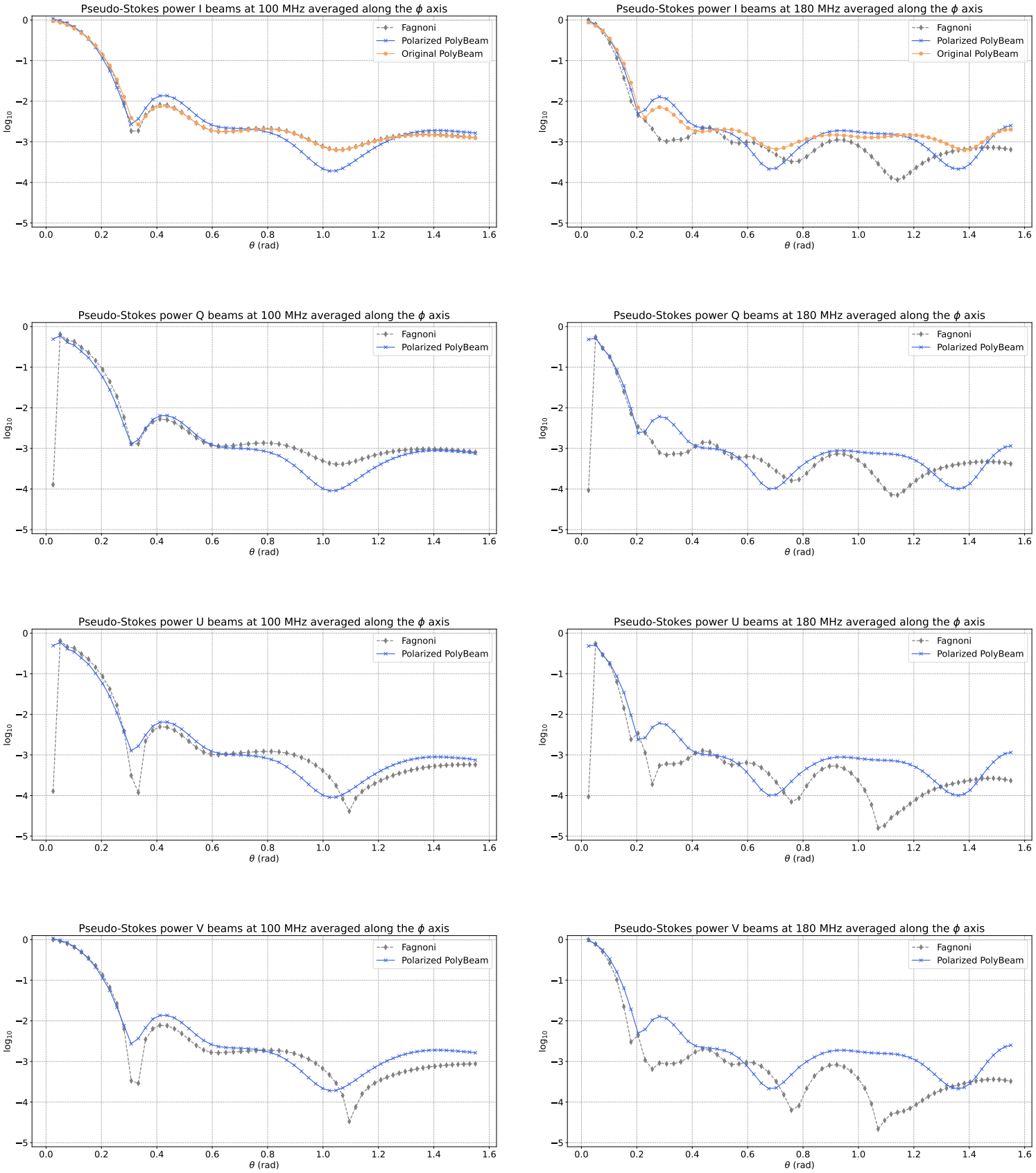

Figure 7: Azimuth-averaged pseudo-Stokes power beams ($\log_{10}$) for pI, pQ, pU, pV polarizations at 100 Mhz (left) and 180 MHz (right).

4 Conclusion

In this memo we found an *ad-hoc* way of deriving complex E-fields at all frequencies and polarizations from an analytical approximation of a real power beam at one frequency and polarization. The operation consisted in modulating the original approximation with a zenith, azimuth, and frequency –dependent complex "dipole matrix" that eventually rendered *de visu* satisfying results, and acceptable aggregated results. We feel that in order to achieve an excellent analytical approximation of the electric fields computed in [Fag+20], a direct polynomial fitting on these, fully taking into account the frequency and polarization dimensions, rather than on an azimuthally-averaged power beam, should be attempted. We provide several opening references ([Ler+11], [Ler+13], and [BCL17]) on the SKA telescope, notably using Zernike polynomials to represent the beam pattern.

Acknowledgements

I would like to thank Philip Bull, Samir Choudhuri and Hugh Garsden for their greatly insightful feedback, and important help, as well as Eloy de Lera Acedo for providing the opening references.

References

[BCL17] Ha Bui-Van, Christophe Craeye, and Eloy de Lera Acedo. "Main beam modeling for large irregular arrays". In: *Experimental Astronomy* 44.2 (Dec. 2017), pp. 239–258. ISSN: 1572-9508. DOI: 10.1007/s10686-017-9565-y. URL: http://dx.doi.org/10.1007/s10686-017-9565-y.

[CBK20] Samir Choudhuri, Philip Bull, and Nicholas S. Kern. "1D Basis Expansion Models for the HERA Primary Beam". Apr. 2020. URL: https://reionization.org/wp-content/uploads/2013/03/HERA081_HERA_Primary_Beam_Chebyshev_Apr2020.pdf.

[Fag+20] Nicolas Fagnoni et al. "Understanding the HERA Phase I receiver system with simulations and its impact on the detectability of the EoR delay power spectrum". In: *Monthly Notices of the Royal Astronomical Society* 500.1 (Oct. 2020), pp. 1232–1242. ISSN: 1365-2966. DOI: 10.1093/mnras/staa3268. URL: http://dx.doi.org/10.1093/mnras/staa3268.

[Gar] Hugh Garsden. *PolyBeam Tutorial*. URL: https://hera-sim.readthedocs.io/en/latest/tutorials/polybeam_simulation.html?highlight=PolyBeam#PolyBeam-Tutorial.

[Ler+11] E. de Lera Acedo et al. "Compact representation of the effects of mutual coupling in non-regular arrays devoted to the SKA telescope". In: *2011 International Conference on Electromagnetics in Advanced Applications*. Sept. 2011, pp. 390–393. DOI: 10.1109/ICEAA.2011.6046372.

[Ler+13] E. de Lera Acedo et al. "Low order beam models for the calibration of large aperture arrays for radio astronomy; The case of the SKA-low instrument". In: *2013 International Conference on Electromagnetics in Advanced Applications (ICEAA)*. Sept. 2013, pp. 1182–1185. DOI: 10.1109/ICEAA.2013.6632431.